IJISET - International Journal of Innovative Science, Engineering & Technology, Vol. 1 Issue 3, May 2014.
www.ijiset.com
ISSN 2348 - 7968

Advanced Driver-Assistances systems With Vehicle Lateral Displacement Using Front Sensors

Mathi.G,Guide Miss S.Saraswathi,
PSN College of Engineering and Technology, Tirunelveli, Tamil Nadu, India

Abstract:- An automated steering control system for passenger carsis analyzed.ADAS using displacement of lateral control system for fornt sensor and GPS. Has been evaluated using system simulations. They have been following different Types:1.The steering angles can be estimated.Type:2 The road curvature estimator for real time situations is design based on its relationship with the steering angle. Type:3 The vehicle's lateral displacements with respect to the road is accomplishes.The proposed estimation and control algorithms are valiated by system simulation result.They show that this lateral steering control system achieve good and robust rformance for vehicles to follow a reference path.

Index Terms-Automated steering control system,lateral displacement,front sensors,GPS,feedback contrl,lateral position estimator.

I. INTRODUCTION

OVER the last decade,road traffic has been constantly increasing,resulting in frequent traffic congestions and a decrease in dfriving safety.Developing advanced driver-assistance systems to reduce crash involvements would benefit millions of people across the world.These developments have resulted in a number of experience system, such as automated highway systems (AHSs),in-vehicle navigation system, breake system steering system,position detection system,vehicle dynaic control system.AHS is an one of the most important types of ADAS.AHS has been investigated byna number of different groups,such as the National Automated Highway Systyem Consortium in the United States,Intelligent Transports Systems(ITS)Japan ,and California PATH in the United States.

They have been into two basic tasks for vehicle control within an automated highway system (AHS).vehicle longitudinal control and vehicle lateral control.this paper is concerned with longitudinal control includes the purpose of length cost in vehicles is to set and maintain the desired speed of the vehicle.The longitudinal control has an important role in platooning control and obstacle avoidances,having the pur[pose of keeping the safe distance between vehicles and of stooping the vehicle in case of a dangers obstacle detested.thus ,also for longitudinal control is reguested a refresh rate 50 Hz and an accuracy in speed control of 0.3 m/s(~1km/h).Finally automated brake system must also implements parking breake functionality, home the break –by-wire contro; system must be available and working also when the vehicles is switched-off and current is not supplied. On the other hand, lateral control includes the purpose of the lateral control system is to steering a moving vehivle automously to satisfy some lateral position demand. A lateral control system is shown in fig: lateraral control algorithm receives environment information,for e.g,from lane markings,magnetic strips or GPS coordinates and vehicles dynamics measurements.(ie vehicle speed yaw rate) and controls the steering system in order to satisfy the demanded lateral position..

Lateral control strategies can be into two types: look-ahead and look-down reference systems.Look-ahead reference systems replicate human driving behavior by measuring the lateral displacement ahead of the vehicle.The Look-ahead distance usually is increased with increasing velocity. A number of research groups have successfully conducted highway speed experiment with Look-ahead system like machine vision.Look-down reference systems the lateral displacement at a location within or in the close vicinity of the vehicle boundaries,typically straight down from the front bumper of the vehicles.(e.g,magnetic marker reference system and electric wire0. these system ave the advantages of beging reliable,yielding accuracy and good performance under any weather or light conditions.onthere one advantages vehicles will not close the lateral displacement –sensing signal.one of most automatic steering control system based on look-down reference system file in te literature can achieve only a small speed of less than 30 m/s~55 mi/h.

To extend the look-down reference systems to experience system conditions of an AHS enviromnt with igh peed above 40 m/s(~65 mi/h).Introducing GPS as an aid for enhancing AHS is not a new concept.several investigations have been done in this field.This papers considers the use of absolute positioning GPS.This proposed estimation and smoothing algorithm are evaluated in computer simulation.

ISSN 2348 - 7968

II.VEHICLE DYNAMIC MODEL

A.Single-Track model

Also, this section describes the vehicle dynamics of a single-track model, which lumps the two wheels of each axle into one wheel.Fig. 1 shows that a vehicle following a lane reference (Zref). The distances from the front wheel and the rear wheel to the CG are ltf and ltr , respectively. For the proposed look-down eference system, the front lateral displacement of the vehicle from the lane reference dsf is measured by using an actual sensor at the front bumper. dsr corresponds to the rear lateral displacement. Since the rear sensor does not exist at the rear bumper, dsr is not available but can be viewed as a measurement by a "virtual sensor.

The model variable denote by:

-The sensors are mounted at lsf in the front of and lsr behind the CG.

-The curvature of the reference track is ρ

-The reciprocal of the track radius R.

- The steering angle is δf

-The side slip angle represents β

- The heading orientation is ψ

- The velocity of the vehicle is v. Thestate space representation for the single-track vehicle dynamic follows the four-order model.

If the lateral displacements are considered into the two state variables (dsf and dsr), the state space function for the single-track model can be represented in another form obtained by applying a transformation from (1). This new methods is representation an

The method following into description types:

*The aforementioned auxiliary variables m;

*The total vehicle mass;

* The total yaw moment of inertia is I.

*Tthe front and rear tires are cf and cr , respectively.

*The road adhesion factor is μ.

They have been into 2 model is represent as :The first vehicle model is used to design the steering angle observer, and the second one is used to develop the lateral displacement estimator. The values of the vehicle's parameters used for the subsequent designs of steering angle observer, displacement estimator, and controller are based on a 1986Pontiac 6 which is an experimental vehicle used by the California000 STE sedan PATH program .

B.Actuator model

The actuator model of the Pontiac 6000 STE sedan is formulated as a third-order low-pass model, which one is used to generate the steering angle δf . A low-bandwidth actuator is a low-pass solution. Other one is this actuator is considered in the control design phase, and it is a linearized third-order low-pass actuator model, which can avoid excitation and saturation. This actuator has a complex pole pair at 5 Hz with 0.4 damping, and a third pole is at 10 Hz. The transfer function.

.

Parameter	Description	Value
λ	Steering head angle	27°
c_t	Mechanical trail	86.53 $[mm]$
d	See Appendix A	4.5 $[mm]$
c_w	Wheel base	1.08 $[m]$
r_r	Rear wheel radius	0.205 $[m]$
r_f	Front wheel radius	0.205 $[m]$
l_f	Forward distance of the front assembly center of mass relative to the front wheel contact point	-0.1073 $[m]$
h_f	Height of the front assembly center of mass relative to the front wheel contact point	0.4110 $[m]$
Iyz_r	y-z product of inertia of rear assembly, measured about rear center of mass.	0.2204 $[kg \cdot m^2]$
Iyz_f	y-z product of inertia of front assembly, measured about front center of mass.	-0.012 $[kg \cdot m^2]$
Ixx_2	Rear wheel moment of inertia, measured about wheel axis.	0.0431 $[kg \cdot m^2]$

III.SATE ESTIMATION MODEL

A.Relatioship of Road Curvature and Steerind Angel model

This situation that the speed of the car is steady state, the car will trace a round of a certain radius (R) if the steering angle value is aconstant. The vehicle path curvature is the reciprocal of the road radius. In [27], it has been proven that the vehicle path curvature can be estimated via two methods: 1) the least squares method and 2) a method based on the mathematical representati information of the steering angle is needed. On the contrast, the on of the vehicle model. In this paper, we select the former one "linear-squares fitting method," in which only information of the steering angle is needed. On the contrast, the information of yaw angle and yaw rate is needed if the second method is adopted. Generally, the estimation of yaw angle and yaw rate is more difficult into implement than the estimation of steering angle. By contrast, the selected method has the advantage of simple and fast computation, thereby yielding easy implementation. Since the vehicle will accurately follow the road geometry in a steering control system, the vehicle path curvature can be approximately viewed as road curvature [20].

Therefore the road curvature is approximately equal to the reciprocal of the road radius ($\rho \approx 1/R$). The relationship

ISSN 2348 - 7968

between the road the road radius ($\rho \approx 1/R$). The relationship between the road curvature and the steering angle (δf) is nearly a straight line according to [27] and the aforementioned approximation. It can be approximated as

$$\rho = \alpha + \gamma \delta f \quad (4)$$

where α and γ are constant parameters. α and γ can be determined through repeated independent simulations (e.g., 500 times). The vehicle model used in these simulations employs the first two variables: sideslip angle and yaw rate (β and r) in (1). Therefore, the front wheel steering angle δf is the only input. The subsystem of the model of (1) is

We introduce the coordinates of the vehicle position to calculate ρ. The derivative of the vehicle position coordinates are

$$X = v\cos\beta \quad (6)$$
$$Y = v \sin \beta \quad (7)$$

Therefore, the entire vehicle dynamic is formed from the combination of (5)-(7), with the following nonlinear state space representation:

ρ can be calculated by the following expression:

During the independent simulations, the values of the steering angle δf are randomly chosen. Based on the road curvature and the steering angle experimental data used or obtained in the independent simulations, the unknown parameters α and γ can be calculated by using the linear least-square estimation method [28]. Then, the linear relationship between the road curvature and the steering angle is determined. If the steering angle is already estimated ($\hat{\delta f}$), the road curvature estimation $\hat{\rho}$ is realized according to their linear relationship.

$$\rho = \alpha + \gamma \hat{\delta f} . \hat{} \quad (10)$$

B. Steering Angle Estimation model

Consider the front displacement dsf and the heading angle ψ as the outputs of the model in (1), the plant is described as

$$\dot{X} = AX + B1\delta f - B2\rho ref$$
$$y = CX \quad (11)$$

with

It is assumed that the second-order derivative of the steering angle is zero ($\ddot{\delta f} = 0$). The reference road curvature input
adopts the linear expression

$$\rho ref = \alpha + \gamma \delta f . \quad (12)$$

Furthermore, we introduce two additional state variables: thefirst-order δf and second-order δf . The model in (1) is then
extended to a new six-order system that has no input signal

$$\dot{XE} = AEXE - BE$$
$$y = CEXE \quad (13)$$

with

X, A, B1, and B2 are defined in (1), and C is defined in (11). Since the steering angle δf is currently one of the state variables, its value can be estimated by a state observer. Such continuous-time observer for the aforementioned six-order extended model has the following structure:

$$\dot{E} = AE \hat{XE} - BE + L(y - CE \hat{E}). \quad (14)$$

XE is the estimation of the vehicle states $\hat{}$

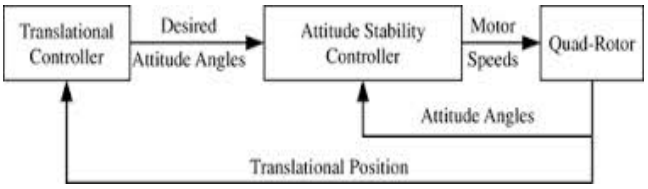

Fig:1Implementation of closed-loop system

The continuous-time vector y is produced by two first-order holds used to interpolate the discrete measurement vector $y*$. $\psi*$ corresponds to the discrete value of the vehicle's heading angle, and $d*sf$ is the discrete value of the vehicle's front lateral displacement

In a real situation, $d*f$ is the discrete measurement from the front sensor. However, $\psi*$ is not the direct measurement of the heading angle from the GPS since the measurements of the heading angle provided by GPS are the values for the geographic coordinate system. To obtain the heading angle for vehicle oordinate system $\psi*$, the GSP measurement of the heading angle at the initial point of a vehicle (origin of the vehicle coordinate plane) should be used as reference. For example, $\psi*$ is the difference in GPS measurements of the
heading angle between the current position and the origin of a vehicle. During simulation, $d*$ f is a simulated discrete value of the vehicle's front lateral displacement. We assume that the GPS measurement of the heading angle for the initial position of a vehicle is 0° . $\psi*$

ISSN 2348 - 7968

corresponds to the simulated discrete value of the vehicle's heading angle.

To choose the optimal gain (L), this state observation problem is solved by solving its dual problem. Here, the linear quadratic regulator theory is applied [29]. An accurate estimation of the steering angle ($\hat{}\delta f$) is obtained from the fifth variable of $\hat{}XE$. Correspondingly, the estimation of the actual road urvature is given by

$$\rho = \alpha + \gamma \hat{}\delta f \,.\, \hat{} \qquad (18)$$

C. Lateral Displacement Estimation

The front and rear lateral displacements (dsf and dsr) must be estimated to design the steering feedback controller. The front sensor measures the actual front lateral displacement with respect to the road ($d* f$). Based on the single-track vehicle model in (2), the estimator has the form

$$H=[1\ 0\ 0\ 0] \qquad (21)$$

U is composed of the estimate of the steering angle ($\hat{}\delta f$) and the actual road curvature ($\hat{}\rho ref$), and they are provided by the estimators in Section III-B

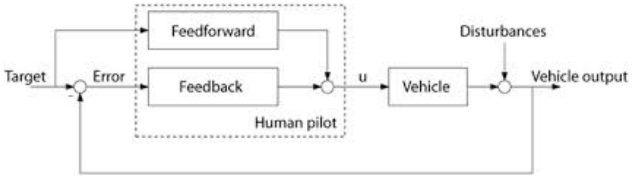

Fig:Block diagram of a a lateral displacement system
dsf is the output of a first-order hold used to interpolate $d*f$,

which is the discrete measurement of the front lateral displacement provided by the front sensor.The proportional gain L is defined as

$$L=l[1\ 1\ 1\ 1] \qquad (23)$$

L is chosen to achieve a small estimation error, and l is gain scheduled with respect to the vehicle . The estimator (16) allows for the estimation of the front and rear lateral displacements ($\hat{}sf$ and $\hat{}sr$). Note that $\hat{}sf$ can be viewed as the actual measurement from the front sensor, which physically exists. In addition, dsr is the measurement from a "virtual rear sensor," which does not physically exist.

IV. Lateral Control Design

A. *System Block Diagram:*

A block diagram of the lateral steering control system using the front and rear displacements (dsf and dsr) as feedback is introduced in [19] and [20], which is shown in Fig. 2.Fig. 3shows the implementation of the entire closed-loop lateral steering control system proposed in this paper. The model for the car and actuator controller dynamics are described in (1) and (3). The boxed pad in

B. Feedback Controller Structure

The feedback controller structure in Fig. 3 was originally developed in [20]. This controller was verified in an experimental test series at California PATH. Such controller is employed in [19] and proven to be suitable and robust. Our system also ploys such controller. The controller structure has three poles,
which could prevent the displacement measurement noise from propagating through the closed-loop system.

V. Simulation Results

Based on the mathematical representation of the vehicle models (1) and (2), the observer is with respect to the vehicle's linear velocity and road adhesion. The observer becomes time varying if velocity and road adhesion are time varying

A Simulation Methodology

The state estimator and feedback controller described.inFig. 3 have been implemented in computer simulations using the model of the Pontiac 6000 STE sedan. It is assumed that GPS has a sampling rate at 1 s. To test the robustness of the controller for actual situations, simulations.of the GPS and the sensor signals are carried out by introducing noises. The measuring noise of GPS is normal distribution with a mean of 0° and a variance of 1 degree2 or N (0, 1). The measuring noise of the displacement sensor is normal distribution with a mean of 0 cm and a variance of 1cm2 or N (0, 1).

The reference road curvature used in simulations is the same as that in [19] and [20], which enables us to compare our results with the results obtained in [19] and [20]. This reference path consists of a straight section, a right turn followed by a left turn, another right turn, and finally a straight section, as shown in Fig. 4. There are no transitions between the curves to obtain the step response. The radius of each turn is Rref = 800m, which means that the road curvatures for each turn is $\rho ref = 1.25 \times 10{-}3$

/m. The simulation takes 60 s for the case of a constant vehicle speed. In the following simulations, four different test cases are conducted for confirming the validity of the proposed GPS/front sensor-based steering control system.

The parameters used for such four test cases are listed in ever, the observer can be considered as time invariant in case that velocity and road adhesion are constant. In this paper, four cases are simulated under two different speeds and two road adhesion conditions (see Table II). During each simulation case, vehicle speed and road adhesion are kept at a constant value. Therefore, the observer gain can be fixed as *a priori* before each simulation. The realization of the observers is given here.

1)The observer gains (L and L) are properly preselected before each simulation case based on the certain constant

speed and road adhesion factor.

2)During each simulation case, the vehicle speed and road

factor are kept at constant values. Then, the observer gains (L and L) are fixed.

This realization method is also employed in [19].

Fig. 5 shows the controller performance on a dry road with a speed at v = 45 mi/h. The estimation results of both steering angle and road curvature are within the accuracy specifications. The root-mean-square error (RMSE) value of steering angle estimation is 8.84%, and the RMSE value of road curvature estimation is 9.98%. Both of these two estimates are quite accurate. The yaw rate is under an acceptable level. The lateral displacement control result has no overshoot and is well damped. This simulation result yields very small maximum vehicle lateral displacement (steady-state error is approximately 0.1 m), which shows extremely accurate road-tracking performance.

To test the performance of the control system on a highway, the simulations are implemented with a speed at v = 80 mi/h. Fig. 6 shows the controller performance on a dry road with a speed of 80 mi/h. The RMSE value of steering angle estimation is 9.13%,and the RMSE value of road curvature estimation is 11.28%. The value of maximum lateral displacement (steady-state error) for each turn is bigger than that in Fig. 5, but it is still small (≈0.2 m). The overshoot of the yaw rate at a higher speed is larger than at a lower speed but still at an acceptable level. all controller gains halved, the lateral displacement increases accordingly compared with the result using the same speed but on a dry road, as shown in Fig. 5.

The RMSE value of steering angle estimation is 10.58%, and the RMSE value of road curvature estimation is 12.26%. The steady-state error of lateral displacement is approximately 0.2 m.The controller performance with a highway speed at v = 80mi/h on a wet road ($\mu = 0.5$) is shown in Fig. 8. The RMSE value of steering angle estimation is 11.54%, and the RMSE value of road curvature estimation is 13.37%. The steady-state error of lateral displacement increases, compared with those in Figs. 6 and 7. The yaw rate result yields a large overshoot nearly 150%, which means that it is unsafe and uncomfortable for passengers to drive on a wet road with a highway speed.

This problem has been discussed in [19], in which the smooth curvature algorithm created from the offline actual road curvature database is applied to improve control performance.

As mentioned before, very large sudden changes for curvature transition are introduced into the lateral control system presented in [19]. Our results, when compared with the results of [19] on the same simulation cases, clearly have smaller steering angle and yaw rate overshoots. Consequently, our control strategy can clearly provide more comfortable and safer ride experience. Only for the worst case (when driving at a highway speed on a wet road) will we need to use some smooth curvature algorithms to ensure high performance.

VI. SUMMARY

In the proposed system, accurate and real time estimations of a vehicle steering angel,road curvature, and a vehicles front and rear lateral displacement have been accomplished.The performance of the steering angle extended observer,The results will be steering control system is implemented using for automated steering control on both dry and wet roads undetr a high vehicle speed.

We narrate the performance of the schedulability test of each task set by the admission control based on the task, which is arrived.

4.1Processor Density and Server Size Assignment

Assigning the density of a processor and server size of each task is an NP-complete problem and it should be resolved to a bin- packing problem. Prior to the consumption of each core as mentioned, initially define the ratio of the number of available subtask consumption in the processor to the number of subtask consumption in the coprocessor.

ISSN 2348 - 7968

$$= \sum_{t_{i,j} \in processor} \frac{c_{i,j}}{D_I} : \sum_{t_{i,k} \in coprocessor} \frac{c_{i,k}}{D_i} \qquad (3)$$

Similarity, the quantiable bandwidth for subtasks in the Processor is the ratio of subtasks in the execution time of the available number of task processor to the relative deadline assigned.

$$\sum t_{i,j} \in processor c_{i,j} \qquad (4)$$

$$(Di - Bi) \chi \frac{u_{processor}}{u_{processor} + u_{coprocessor}}$$

The heterogeneous dual-core scheduling algorithm normally used to timing constraints and the worst case computation time. We calculate computation time, there are a lot of results in previous research, and the server size of the coprocessor can be differently adapted by feedback control schemes and probability queuing mechanisms. With the available adapted server size, the heterogeneous dual-core scheduling algorithms and admission control can also be extended for uncertain computation time.

4.2 Sufficient Schedulability Test

We narrate the admission control of the heterogeneous dual-core scheduling algorithm the schedulability test is categorized into three major divisions. They are processor consumption test, coprocessor consumption test and deadline based on task test.

V. HETEROGENEOUS MULTICORE SCHEDULING ALGORITHM

The scheduling problem on homogeneous multicore algorithm is dispatched as completed no preemption problem. Using separation module, all jobs of a specific task executed on the homogeneous coprocessor.

Fig 5a.Global schema illustrates the proposed module of subtask in the coprocessor and is received by its related server. Each subtask is ready with that of instances, the related server sets the fixed value of deadline and push it ready to queue in a global manner.

Fig 5b.Partition schema illustrates that the server is represented to the coprocessor. The instance related to this coprocessor is inserted into the queue as ready with that of a sporadic activity.

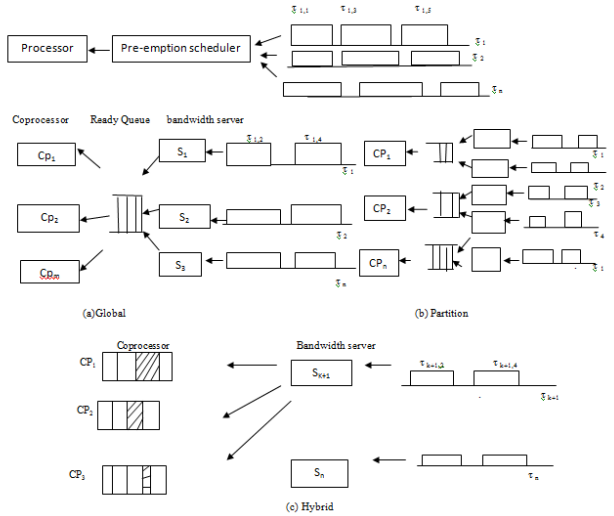

Fig. 5. Heterogeneous multicore scheduling framework.

Fig 5b.hybrid schema is assumed as various server and are separated to that particular coprocessor among the processor. The details of the separated schematic rule are not illustrated in this figure. The corresponding coprocessor and the remaining servers between coprocessors, subtasks might be split.

VI. PERFORMANCE EVALUATION

In real time application we presented the practical section of the proposed module. The extended work of the heterogeneous dual-core scheduling algorithm –based on global, partition and hybrid dispatching rules for heterogeneous multicore systems is demonstrated using adaptable dispatchers.

6.1 Experimental Setup

The evaluation of the Heterogeneous dual-core scheduling algorithm is compared with that of Earliest Deadline First algorithm, Rate Mono- tonic scheduling algorithm(RM),scheduling rule using Priority Ceiling Protocol(PCP) [2], and Stack Resource Protocol (SRP) scheduling algorithms.

6.2Experimental Results

We narrate the experimental results using different task sets and compare our Heterogeneous dual-core scheduling algorithm against rate monotonic scheduling algorithm and earliest deadline first algorithm, and against a scheduling rule using priority ceiling protocol and a stack resource protocol in the following subsections in 6.2.

6.2.1 Synchronization Protocols versus

ISSN 2348 - 7968

Schedulers

We illustrate the performance of heterogeneous dual-core scheduling algorithm with a nonpreemptive. Are measured for 55 random number of generated task sets to evaluate the average numbers of errors. Initially the performance metric is the completion ratio, which means for the ratio of the total number of available task sets to the total number of all given task sets. After the Evaluation, the performance ratio is better when completion ratio is higher. All the available task sets in the experiments for this performance measurement are randomly generated for a specific consumption without schedulability test.

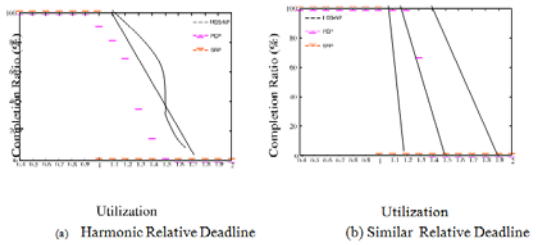

Fig. 6. Completion ratios of protocols under varied task utilizations.

Coprocessor. Fig. 6 shows the completion ratios for using Synchronization protocols, such as Priority Ceiling Protocol, Stack Resource Protocol, or the Heterogeneous dual-core scheduling algorithm non-pre-emption points, with different total consumption of tasks. When PCP and SRP are used, tasks are scheduled into the processor by Rate Mono- tonic and Earliest Deadline First algorithm schedulers, respectively. A task executing on the coprocessor is nonpreemptive in this experiment. The U and V-axis represents the total utilization of tasks and the completion ratio. In fig 6a and 6b the relative deadline available task sets are harmonic and same. Comparing both the cases stack Resource Protocol performance is not better than Priority Ceiling Protocol due to its HDS-NP critical section.

Fig. 7 shows the completion ratios using dispatchers by scheduling algorithm, such as RM, EDF, and the HDS algorithm under different total consumptions of tasks. Compare the performance evaluation of fig7a and 7b the performance of Rate Mono- tonic scheduling algorithm is better due to the setting of harmonic relative deadline and then comparing Figs. 6b and 7b, the Priority Ceiling Protocol's performance is better than the Rate Mono- tonic scheduling algorithm.

6.2.2 Varying Pre-emption Point Intervals and Context Switch Overhead

In this section, utilization using synchro nization protocols is worse, thus we compare Heterogeneous dual-core scheduling algorithm with other dispatchers. Illustrates the completion ratios of Rate Mono- tonic scheduling algorithm, Earliest Deadline First algorithm, and Heterogeneous dual-core scheduling Algorithm under various interval of the preemption point. The U-axis represents the interval of the pre-emption point, and the V -axis represents the completion ratio. When pre-emption interval increases, completion ratio decreases under Earliest Deadline First algorithm and Heterogeneous dual-core scheduling algorithm as shown fig 8a. This is due to the shorter relative deadline to leave its timing constraint with the longer non preemption portion generates the task sets.

6.2.3Real-Life Applications

We exhibit, Rate Mono- tonic scheduling algorithm, Earliest Deadline First algorithm, Heterogeneous dual-core scheduling algorithm, Priority Ceiling Protocol, and Stack Resource Protocol on the processor. When Rate Mono- tonic scheduling algorithm and Heterogeneous dual-core scheduling algorithm are used, a task queue is implemented on the coprocessor. When Priority Ceiling Protocol, and Stack Resource Protocol on the processor and are used, all the executed tasks on the coprocessor are without preemptive.

The estimated response time of each task is evaluated in the scenario as given below. To business uses on a smart phone and several news videos on a video phone are executed simultaneously. Motion JPEG decoding processes are embedded in the above application and are evaluated under testing at a resolution of pixel rate 720 x 240.Utiliation of processor is used for controlling the event inputTask and output task and the coprocessor is used for decoding calculations. The Communication of processor and the coprocessor is achieved by the quality of service and mailbox. The buffer size in input and output is 16 KB. Each task set has three subtasks. The first and second task performs the

ISSN 2348 - 7968

input and output control, respectively, and both are executed on the processor. The second task in the subtask performs the decoding computation and is execute on the coprocessor. The computation time of each and every subtask is estimated by exhaustive profiling. In this experiment, the input and output control functions executed on the processor takes 9.9 and 1.5 ms, respectively. The decoding function is executed on the coprocessor in 18 ms. There are two pre-emption points inserted in the decoding function. Decoding process based on JPEG is not an application based on hard real time, but it is the constraint based on the real time process due to quality of service. Utilizing various quality-of-service, arranging the decoding processes through Motion JPEG, for evaluating algorithmic performance. More frames per second(FPS) indicates a good quality of service, and the assumption of dropped frames are not critical. Given a task set with frame rates of 35, 25, 15, and 4 FPS, the task set is not schedulable using SRP and PCP, and the performances of the schedulers (HDS, EDF, and RM) are similar. With frame rates 11, 8, 5, and 5 FPS, using the task set is executed heterogeneous dual-core scheduling algorithm. The experiment results reveal that when the coprocessor is assumed to be fully pre-emptive, HDS improves the frame rate of this task set from 4 to 8 FPS as compared to the scheduler implementations (RM and EDF). Compared to the protocol implementations,HDS improves the frame rate from 4 to 25 FPS.3 Assumption of our frames which are all dropped are not critical. Given a task set with frame rates of 25, 10, 5, and 4 FPS, the task set is not schedulable using SRP and PCP, and the performances of the schedulers (HDS, EDF, and RM) are similar.

With frame rates 25, 10, 8, and 5 FPS, the task set is only schedulable using HDS. The experiment results reveal that when the coprocessor is assumed to be fully pre-emptive, HDS improves the enhancing frame rate of subtask set from 4 to 8 FPS as compared to process is not a hard real-time application, the real-time constraint of the process is due to the quality-of-service requirement in the system. Assumption of our frames which are all dropped are not critical, based on the performance evaluation. Given a task set with frame rates of 25, 10, 5, and 4 FPS, the task set is not schedulable using SRP and PCP, and the performances of the schedulers (HDS, EDF, and RM) are similar. With frame rates 25, 10, 8, and 5 FPS, the task set is only Schedulable using HDS.

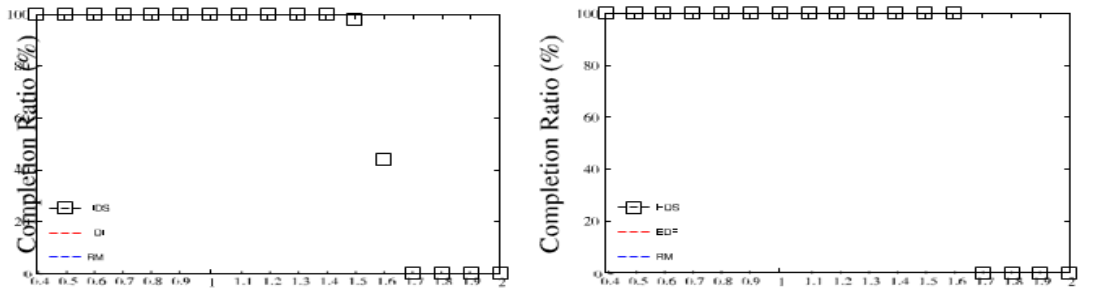

(a) Harmonic Relative Deadline (b) Similar Relative Deadline

Fig. 7. Completion ratios of schedulers under varied task utilizations.

6.2.4 Multiple Coprocessors with Varied Dispatchers

In this system one processor and multiple coprocessors, because most heterogeneous multi- core systems are equipped with multiple coprocessors to accelerate task executions. We implemented Heterogeneous dual-core scheduling algorithm based on first fit, worst fit, Global, and Hybrid dispatchers on a system with one processor and three coprocessors and then first fit and worst fit dispatchers partition tasks by the maximum needed server. The global dispatcher always dispatches the job with the shortest deadline assigned by Heterogeneous dual-core scheduling algorithm into the coprocessor. The hybrid dispatcher first assigns tasks to the particular processors according to the first fit.

ISSN 2348 - 7968

VII CONCLUSION

The contributed work of this paper explains the real-time task, dispatching errors in different coprocessors and deals with the timing and priority constraints without pre-emptive execution of tasks. Initially propose the schedulability test by the acceptance of changing the value of each jobs. An inversion pre-emption point based solution is depicted as the configuration of overhead mechanisms and bounding capability in the coprocessor the extended mechanism of different coprocessor is achieved by using adaptable schedulers.

Results obtained by various experiments are observed by the evaluation of scheduling rules under varying jobs and tasks. Future work related to the online efficiency mechanisms of different coprocessor

and consumption bounding and blocking time different coprocessor. Enhancing various pre-emptive mechanisms will tend to the development of design in mobile system utilization.

REFERENCES

[1]Qualcomm,Inc.,"Snapdragon,"technical report,Qualcomm.http://www.qualcomm/media/documets/snapdragon-s4-processors-system-chip-solutions-new-mobile-age,2011 report.

[2] L. Sha, R. Rajkumar, and J. Lehoczky, "Priority Inheritance Protocols: An Approach to Real-Time Synchronization," IEEE Trans. Computers, vol. 39, no. 9, pp. 1175-1185, Sept. 1990.

[3] Paolo Gai, Luca Abeni, Giorgio Buttazzo. Multiprocessor DSP Scheduling in System-on-a-chip Architectures. Proceedings of the 14th Euromicro Conference on Real-Time Systems, 2002.

[4] Bautin, M., Dwarakinath, A., And Chiueh, T. Graphics Engine Resource Management. In Proc. MMCN (2008)..

[5]L. Benini, D. Bertozzi, A. Guerri, and M. Milano,"Allocation, Scheduling and Voltage Scaling on Energy Aware MPSoCs," Proc. Conf. Integration of AI and OR Techniques in Constraint Programming for Combinatorial Optimization Problems, 2006.

[6] K.-Y. Hsieh, Y.-C. Lin, C.-C. Huang and J.-K. Lee, "Enhancing Microkernel Performance on VLIM DSP Processors via Multiset Context Switch,"

[7] L. Steffens, M. Agarwal, and P. Vander Wolf, "Real-Time Analysis for Memory Access in Media Processing Socs: A Practical Approach," Proc. Euromicro Conf. Real-Time Systems, 2008.